

Supplementary Information: Harnessing the Power of Microwave for Inactivating *Pseudomonas aeruginosa* with Nanohybrids

Jaime Plazas-Tuttle^{‡,†}, Dipesh Das[†], Indu V. Sabaraya[†], and Navid B. Saleh^{†,*}

[†]Department of Civil, Architectural, and Environmental Engineering, University of Texas at Austin, Austin, TX 78712

[‡]Department of Civil and Environmental Engineering, Universidad de los Andes, Carrera 1 Este No. 19 A-40, Edificio ML, Piso 6, Bogotá, Colombia (Current affiliation)

*Corresponding author: Navid B. Saleh, email: navid.saleh@utexas.edu, phone: (512) 471-9175

Here we provide additional theoretical background on the ROS generation for the proposed mechanism of disinfection in the discussion section, and additional information on the synthesis, characterization of nanohybrids (NHs), and details on assessment of disinfection mechanism.

| CONTENTS: | | Page |
|--------------------|--|----------|
| Table S1. | Loading ratios of the 3 NHs. | 2 |
| Table S2. | EDX elemental composition of the 3 NHs synthesized. | 2 |
| Table S3. | Summary of XPS data and weight % of elements. | 2 |
| Table S4. | Temperature increase after 20 s microwave irradiation time at 10 % power. | 3 |
| Table S5. | ROS generating reactions. | 8 |
| Figure S1. | STEM HAADF images of a representative ion-beam irradiated samples of NH-1. | 4 |
| Figure S2. | STEM images and elemental mapping of the 3 NHs synthesized. | 5 |
| Figure S3. | TGA analysis of representative samples of fMWNT and NHs. | 6 |
| Figure S4. | Delta Temperature after 20 s microwave irradiation time at 10 % power for all the samples. | 7 |
| Section S1. | ROS Generation. | 8 |

Table S1. Loading ratios of the 3 NHs

| No. | Name | Amount of MWNTs | Amount of salt* | Molar Ratio |
|-----|------|-----------------|-----------------|-----------------------|
| | | (mg) | (mg) | (C:Er ³⁺) |
| 1 | NH-1 | 50 | 115 | 16.04:1 |
| 2 | NH-2 | 50 | 230 | 8.02:1 |
| 3 | NH-3 | 50 | 460 | 4.01:1 |

* Erbium salt: Er(NO₃)₃·5H₂O

Table S2. EDX elemental composition of the NHs synthesized.

| Element | Weight %* | | |
|--|-----------|-------|-------|
| | NH-1 | NH-2 | NH-3 |
| Carbon | 41.36 | 23.82 | 7.47 |
| Erbium | 47.91 | 64.12 | 80.11 |
| Oxygen | 10.73 | 12.06 | 12.41 |
| Relative Ratios C:Er³⁺ | 0.86 | 0.37 | 0.09 |

*Weight % calculated as the atomic percentage times molecular weight divided by the total sum of elements detected.

Table S3. Summary of XPS data and weight percentage of elements.

| XPS Region | Weight %* | | |
|--|-----------|-------|-------|
| | NH-1 | NH-2 | NH-3 |
| C 1s | 49.08 | 35.71 | 12.90 |
| Er 4d | 38.16 | 49.35 | 69.13 |
| O 1s | 12.76 | 14.94 | 17.97 |
| Relative Ratios C:Er³⁺ | 1.29 | 0.72 | 0.19 |

*Weight % calculated as the atomic percentage times molecular weight divided by the total sum of elements detected.

Table S4. Temperature increase after 20 s microwave irradiation time at 10% power.

| | Initial Temperature, °C | Final Temperature, °C | Delta Temp, °C |
|-------|-------------------------------|-----------------------------|-------------------|
| DI | 22.10 | 23.27 | 1.17±0.12 |
| MWNT | 23.23 | 24.03 | 0.80±0.10 |
| Salt* | 23.27 | 24.37 | 1.10±0.17 |
| NH-1 | 23.40 | 25.50 | 2.10±0.30 |
| NH-2 | 23.67 | 24.87 | 1.20±0.17 |
| NH-3 | 23.33 | 24.37 | 1.03±0.06 |

* Erbium salt: $\text{Er}(\text{NO}_3)_3 \cdot 5\text{H}_2\text{O}$

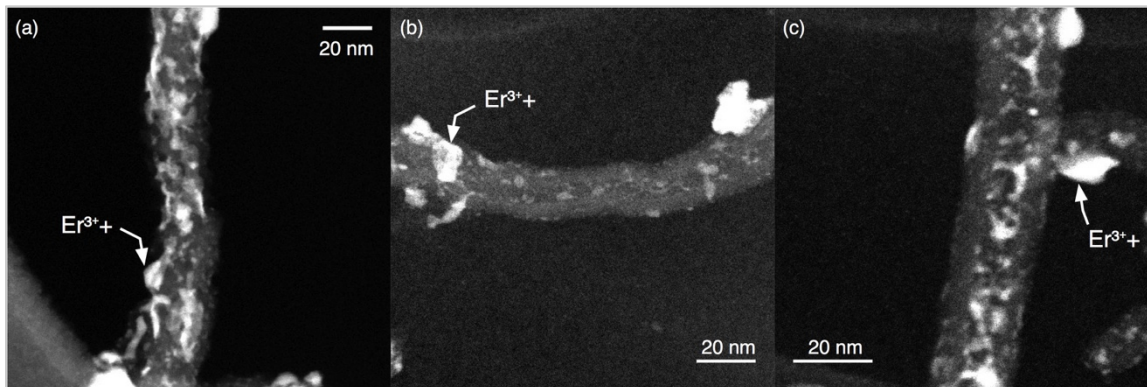


Figure S1. STEM HAADF images of a representative ion-beam irradiated samples of NH-1.

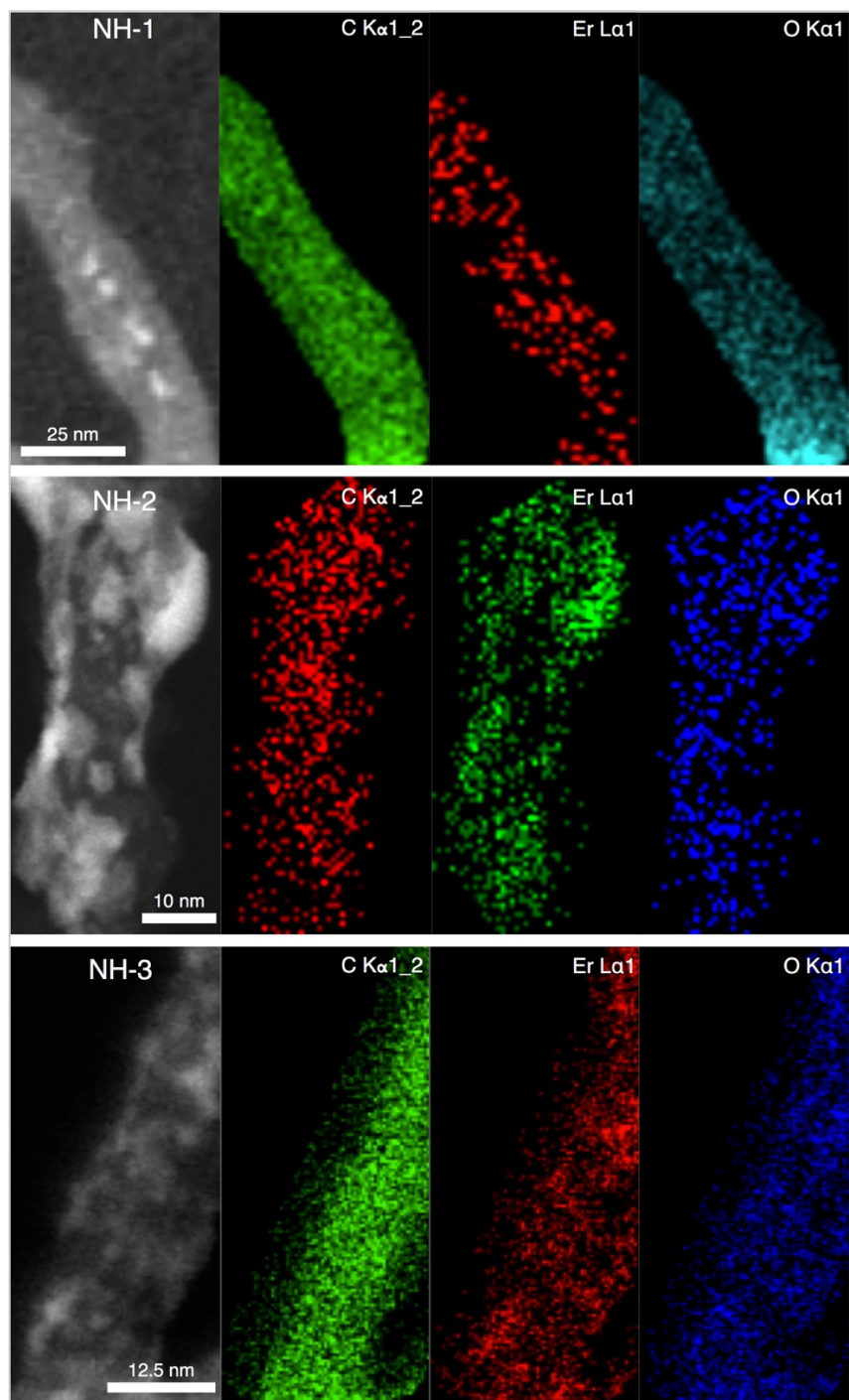


Figure S2. STEM images and elemental mapping of the 3 synthesized NHs.

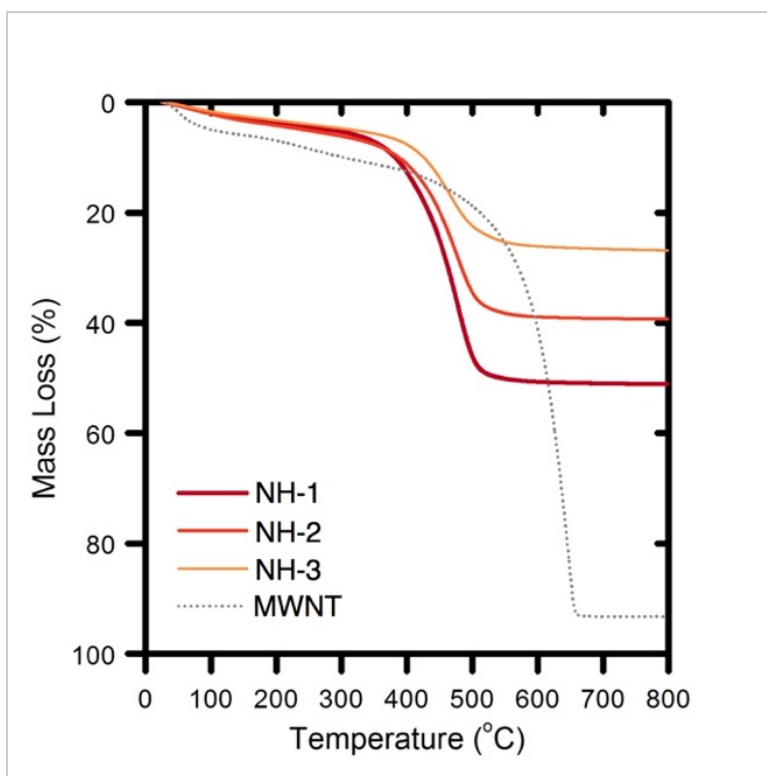


Figure S3. TGA analyses of representative functionalized MWNT and NH samples. Temperatures of oxidation for the NHs are 475 °C (NH-1), 474 °C (NH-2), and 467 °C (NH-3) respectively.

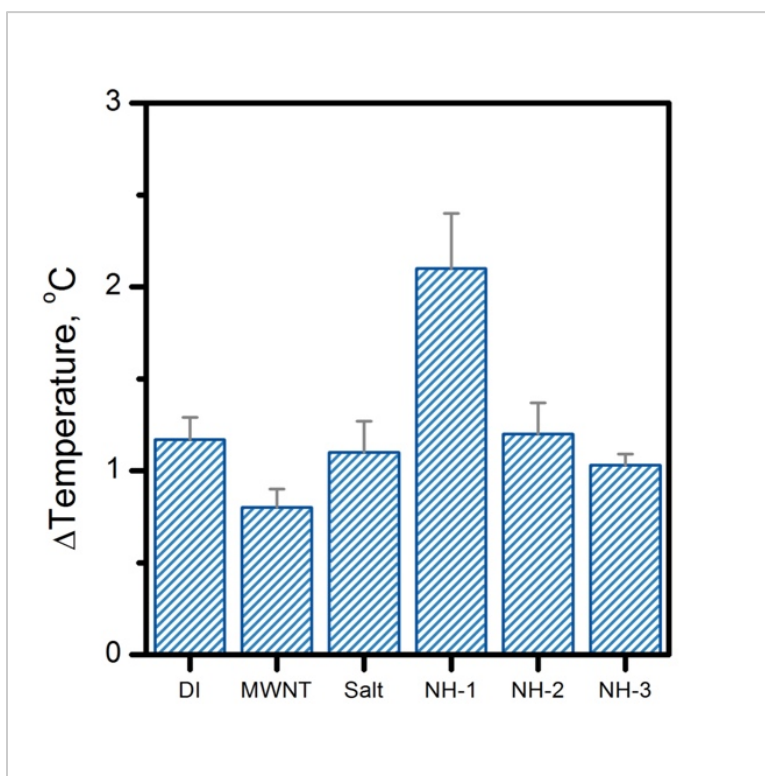


Figure S4. Temperature differences between irradiated and microwave radiated samples. Differences are presented from room temperature (21 °C).

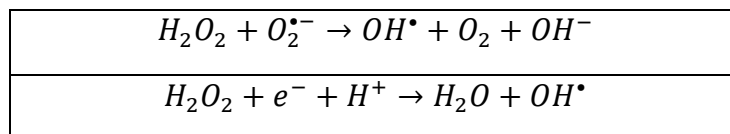
Section S1. ROS Generation

Oxidative stress is one of the key mechanisms causing antimicrobial activity when nanoparticles interact with bacteria (Stone and Donaldson, 2006). Such stresses are caused by an imbalance between damaging oxidants (e.g., H_2O_2 and OH^\bullet) and protective antioxidants (e.g., vitamin C and glutathione) (Stone and Donaldson, 2006) within a nano-bio system. Studies have shown ROS generation from surfaces of metal oxide nanocrystals (Burello and Worth, 2011; Long et al., 2006). Oxygen can be activated to form ROS by both energy transfer and electron transfer processes. The former leads to the formation of singlet oxygen (1O_2), while the latter results in the generation of superoxide ($O_2^{\bullet-}$), which undergoes further chemical transformation in water.

When illuminated, metal oxides such as ZnO (Arguinzoniz et al., 2013) and TiO_2 (Aksel and Eder, 2010), cause charge separation, generating a hole (h^+) in the valence band (E_V) and an electron (e^-) in the conduction band (E_C) (Table S5). Holes extract electrons from water and/or hydroxyl ions, generating OH^\bullet . Electrons reduce O_2 producing $O_2^{\bullet-}$ and other ROS in a cascade of consecutive reactions (Table S5).

Table S5. ROS generating reactions (Buettner, 1993).

| |
|--|
| $metal\ oxide + light \rightarrow h^+ + e^-$ |
| $H_2O + h^+ \rightarrow OH^\bullet + H^+; \quad OH^\bullet + H^+ + e^- \rightarrow H_2O$ |
| $O_2 + e^- \rightarrow O_2^{\bullet-}$ |
| $O_2^{\bullet-} + H^+ \rightarrow HO_2^\bullet$ |
| $O_2^{\bullet-} + H^+ + e^- \rightarrow H_2O_2$ |
| $2HO_2^\bullet \rightarrow H_2O_2 + O_2$ |
| $O_2 + 2H^+ + 2e^- \rightarrow H_2O_2$ |



Studies have shown that 1O_2 can be generated indirectly from metal oxide nanoparticles via the oxidation of $O_2^{\bullet-}$ (Daimon and Nosaka, 2007; Hirakawa and Hirano, 2006) and when sufficient energy capable of reversing the spin on one of the unpaired electrons of O_2 is absorbed, primarily through an energy transfer process (Sharma et al., 2012). Carbon-based photosensitizers (i.e. C_{60} fullerenes) have been shown to absorb UV or visible electromagnetic radiation and transfer it to surrounding molecules, and thereby facilitate energy or electron transfer that lead to the formation of 1O_2 or $O_2^{\bullet-}$, respectively (Brunet et al., 2009). In particular, MWNTs can accept electrons and aid in ballistic transport along MWNT (Vázquez and Prato, 2009) axes, making these carbon structures excellent candidates to scatter electrons with enhanced surface area.

REFERENCES

- Aksel, S., Eder, D., 2010. Catalytic effect of metal oxides on the oxidation resistance in carbon nanotube–inorganic hybrids 20, 9149–9146. doi:10.1039/c0jm01129k
- Arguinoniz, A.G., Ruggiero, E., Habtemariam, A., Hernández-Gil, J., Salassa, L., Mareque-Rivas, J.C., 2013. Light Harvesting and Photoemission by Nanoparticles for Photodynamic Therapy. Part. Part. Syst. Charact. 31, 46–75. doi:10.1002/ppsc.201300314
- Brunet, L., Lyon, D.Y., Hotze, E.M., Alvarez, P.J.J., Wiesner, M.R., 2009. Comparative Photoactivity and Antibacterial Properties of C 60Fullerenes and Titanium Dioxide Nanoparticles. Environ. Sci. Technol. 43, 4355–4360. doi:10.1021/es803093t
- Buettner, G.R., 1993. The Pecking Order of Free-Radicals and Antioxidants - Lipid-Peroxidation, Alpha-Tocopherol, and Ascorbate. Arch. Biochem. Biophys. 300, 535–543. doi:10.1006/abbi.1993.1074
- Burello, E., Worth, A.P., 2011. A theoretical framework for predicting the oxidative stress potential of oxide nanoparticles. Nanotoxicology 5, 228–235. doi:10.3109/17435390.2010.502980
- Daimon, T., Nosaka, Y., 2007. Formation and Behavior of Singlet Molecular Oxygen in TiO₂ Photocatalysis Studied by Detection of Near-Infrared Phosphorescence. J. Phys. Chem. C 111, 4420–4424. doi:10.1021/jp070028y
- Hirakawa, K., Hirano, T., 2006. Singlet oxygen generation photocatalyzed by TiO₂ particles and its contribution to biomolecule damage. Chemistry Letters 35, 832–833. doi:10.1246/cl.2006.832
- Long, T.C., Saleh, N.B., Tilton, R.D., Lowry, G.V., Veronesi, B., 2006. Titanium Dioxide (P25) Produces Reactive Oxygen Species in Immortalized Brain Microglia (BV2): Implications for Nanoparticle Neurotoxicity †. Environ. Sci. Technol. 40, 4346–4352. doi:10.1021/es060589n
- Sharma, P., Jha, A.B., Dubey, R.S., Pessarakli, M., 2012. Reactive Oxygen Species, Oxidative Damage, and Antioxidative Defense Mechanism in Plants under Stressful Conditions. Journal of Botany 2012, 1–26. doi:10.1155/2012/217037
- Stone, V., Donaldson, K., 2006. Nanotoxicology - Signs of stress. Nature Nanotech 1, 23–24. doi:10.1038/nnano.2006.69
- Vázquez, E., Prato, M., 2009. Carbon Nanotubes and Microwaves: Interactions, Responses, and Applications. ACS Nano 3, 3819–3824. doi:10.1021/nn901604j